

Evidence for  $J$  dependence in  $^{60}\text{Ni}(^3\text{He},d)^{61}\text{Cu}$  cross sections

J. E. Kim\* and W. W. Daehnick

*Nuclear Physics Laboratory, University of Pittsburgh, Pittsburgh, Pennsylvania 15260*

(Received 12 February 1981)

The  $^{60}\text{Ni}(^3\text{He},d)^{61}\text{Cu}$  reaction was studied in order to investigate  $j$ -dependent effects at small angles. Absolute differential cross sections were measured in small angular steps over the range  $1.6^\circ \leq \theta \leq 40^\circ$ . A high-resolution position-sensitive (helix) gas counter in the focal plane of a spectrograph was used as a detector. The total energy resolution ranged from 12 to 15 keV. Orbital angular momentum transfers and spectroscopic factors were extracted from comparison with distorted-wave Born-approximation (DWBA) calculations for the levels up to 3.86 MeV in  $^{61}\text{Cu}$ . Many higher-lying  $l = 1$  and 3 and one  $l = 2$  transitions are newly observed. Angular distributions for known  $f_{5/2}$  stripping showed a  $2-3^\circ$  forward shift of stripping peak positions relative to  $f_{7/2}$  transfers. For  $l = 1$  transitions small-angle ( $0^\circ-5^\circ$ ) cross sections of the  $p_{1/2}$  transfers are appreciably enhanced whereas the angular shapes of known  $p_{3/2}$  states are in excellent agreement with the distorted-wave Born approximation. Distorted-wave Born approximation calculations which include spin-orbit effects in the entrance and exit channels do not reproduce these  $j$ -dependent differences.

[ NUCLEAR REACTIONS  $^{60}\text{Ni}(^3\text{He},d)^{61}\text{Cu}$ ,  $E_{^3\text{He}} = 18$  MeV; measured  $\sigma(E_d, \theta)$ , resolution  $\sim 13$  keV. DWBA analysis, deduced  $l, \pi$ , spectroscopic factors, small angle  $l = 1, 3$   $j$  dependence. ]

## I. INTRODUCTION

Single-nucleon stripping and pickup reactions have been extensively used in deriving angular momentum and parity of residual states. However, the orbital angular momentum transfer deduced from such reactions does not, in general, provide a unique assignment of total angular momentum ( $J$ ) for the final nuclear state. In the  $f-p$  shell most low-lying levels have fairly well-established  $l$  values, but there are few reliable assignments of  $j$  values. Many observations have been reported regarding the  $j$ -dependent behavior of angular distributions observed in certain stripping and pickup reactions such as  $(d,p)$ ,<sup>1</sup>  $(p,d)$ ,<sup>2</sup> and  $(d,t)$ .<sup>3,4</sup> More recently it has been found that experimental  $^{50,52}\text{Cu}$  ( $^3\text{He},d$ )<sup>51,53</sup>Mn angular distributions at small angles not only depend on the orbital angular momentum  $l$ , but also on the total angular-momentum transfer  $j$ . The  $J$ -dependent features of ( $^3\text{He},d$ ) cross sections were most easily noticed as differences measured between DWBA predictions (which depend on  $l$  and  $Q$  value) and experimental cross sections

which at small angles, in addition, depend on the  $j$  transfer. An enhancement of the  $p_{1/2}$  cross sections for angles below  $10^\circ$  and a forward shift of the main stripping peak of the  $f_{5/2}$  transitions were observed, while the  $p_{3/2}$  and  $f_{7/2}$  angular shapes were in good agreement with DWBA calculations.<sup>5</sup> Here we extend the study of this small-angle  $j$  dependence of the ( $^3\text{He},d$ ) reaction to the target nucleus  $^{60}\text{Ni}$ , at the beam energy of 18 MeV. Our main interest is to investigate if the  $j$ -dependent differences in the small-angle cross sections persist and are stable for other targets in the  $1f-2p$  shell.

The  $^{60}\text{Ni}(^3\text{He},d)^{61}\text{Cu}$  reaction was studied in 1968 by Pullen and Rosner<sup>6</sup> at 16.4 MeV, with 19 keV energy resolution. In their work  $l_p$  values and spectroscopic factors were obtained for 11 strongly excited levels of  $^{61}\text{Cu}$ . The properties of  $^{61}\text{Cu}$  states have been extensively studied by means of proton capture measurements<sup>7-12</sup> and therefore many of the lower-lying levels have well-established  $J^\pi$  values.<sup>61</sup>  $^{61}\text{Cu}$  thus serves our purpose well in providing many levels with definite spin assignments for the comparison with those deduced from the present study.

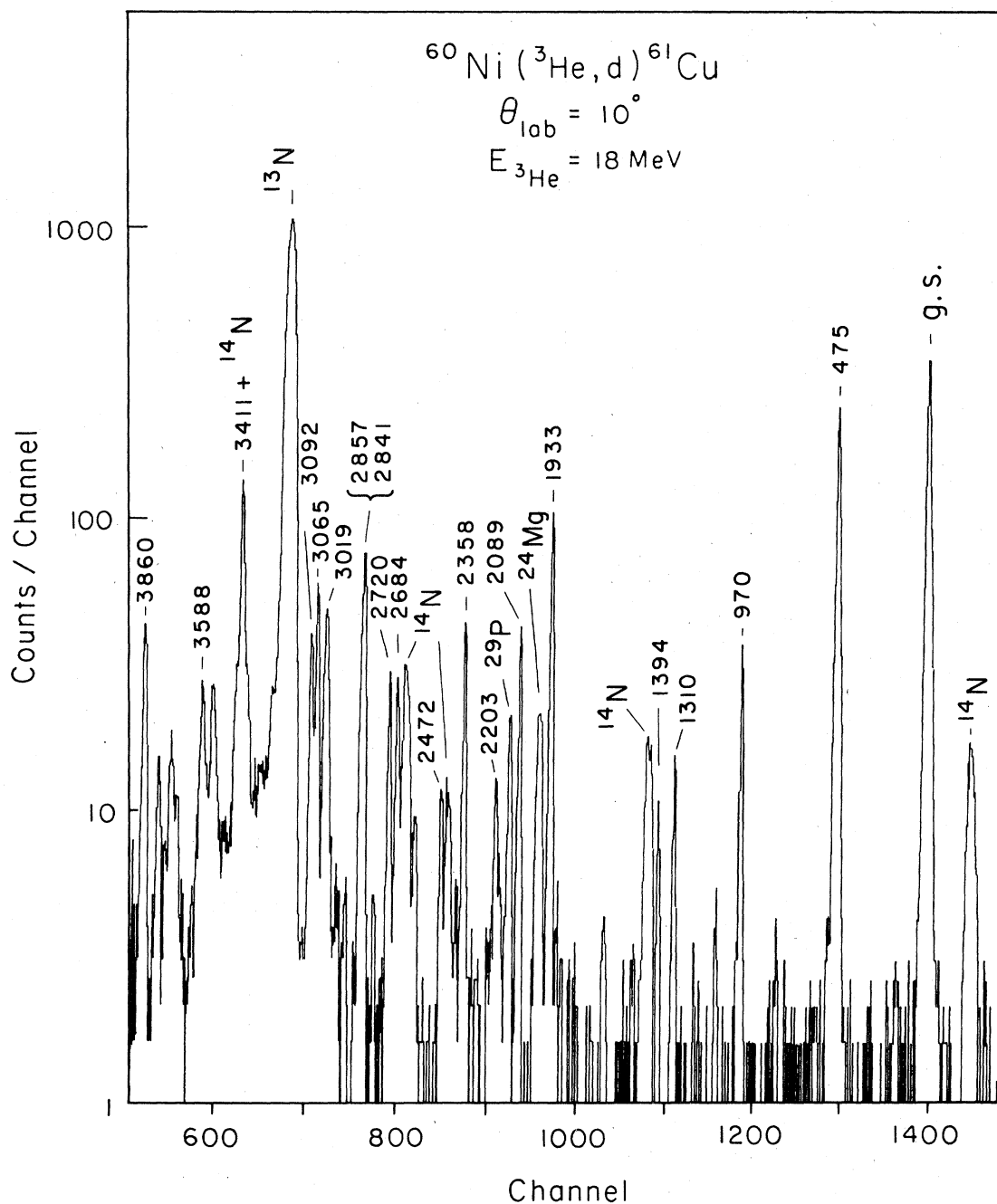


FIG. 1. Semilog spectrum of deuterons from  $^{60}\text{Ni}({}^3\text{He}, d){}^{61}\text{Cu}$  at  $\theta = 10^\circ$  taken with a helix counter. The level energies and spins are from the adopted values in the Nuclear Data Sheets (Ref. 14).

## II. EXPERIMENTAL PROCEDURE

The  $^{60}\text{Ni}({}^3\text{He}, d){}^{61}\text{Cu}$  experiment was performed using an 18 MeV  ${}^3\text{He}$  beam from the University of Pittsburgh Van de Graaff accelerator. The targets

were prepared by vacuum evaporation of metallic  $^{60}\text{Ni}$  onto 6–10  $\mu\text{g}/\text{cm}^2$  carbon backings to thicknesses of about 25  $\mu\text{g}/\text{cm}^2$ . The isotopic purity of the target material was 99.79%. Small amounts of O, Si, Na, Cl, and Cu contaminants were present.

Target thickness was determined by measuring the yield of elastically scattered  $^3\text{He}$  particles from the individual targets at small scattering angles, where the cross section is very close to Coulomb scattering. The beam was monitored by charge collection and, simultaneously, by a measurement of elastically scattered  $^3\text{He}$  ions. The scattering monitors were Si detectors positioned at  $\pm 25^\circ$  relative to the beam direction. Absolute ( $^3\text{He},d$ ) differential cross sections were obtained by normalizing the observed monitor yields to optical-model calculations. The random cross-section uncertainties primarily arise from statistics, background subtraction, and the random monitoring error which was  $\leq 5\%$ . The absolute scale error is estimated to be  $\pm 15\%$ .

The reaction deuterons were momentum analyzed with an Enge split-pole spectrograph and detected at the focal plane with a position-sensitive helical cathode gas proportional counter.<sup>13</sup> Deuteron spectra were obtained at 11 angles from  $1.6^\circ$  to  $40^\circ$  in small angular steps, particularly at forward angles. The data for  $\theta_{\text{av}} = 1.6^\circ$  were taken with the detector set at  $\theta = 0^\circ$ . At this setting the full incident beam would enter the spectrograph and create a large background of x-rays, neutrons, and  $^3\text{He}$  particles of a charge state different from that of the incident beam ( $^3\text{He}^{++}$ ). A very narrow (4 mm) "finger"-shaped beam stop was placed at  $0^\circ$ , 16.8 cm from the target in order to block the direct beam before it entered the spectrograph. It also blocked the central 0.3 msr of the spectrograph solid angle which normally was 1.2 msr. Thus with the spectrograph at  $\theta = 0$  the average reaction angle was  $1.6^\circ$  in the laboratory system. The use of the helix (position,  $\Delta E, E$ ) telescope in conjunction with the Pittsburgh spectrograph was necessary for zero and other small-angle measurements. Considerable background reduction was achieved by requiring a triple coincidence between the position,  $\Delta E$  and  $E$  detectors, and by particle identification with the aid of the on-line computer. The helix spectrum taken at  $\theta = 10^\circ$  is shown in Fig. 1. The energy resolution of this spectrum, 12–15 keV (full width at half maximum) was also typical of the spectra obtained at other angles. Relative excitation energies were extracted, but the absolute energies shown for the excited levels in  $^{61}\text{Cu}$  were taken from Ref. 14. The correspondence was easily established as the ( $^3\text{He},d$ ) reactions on the chromium isotopes<sup>5</sup> using the same helix counter had shown good detector linearity. (The rms deviation of energy measurements was 2–3 keV over the total length of the counter.)

### III. ANALYSIS AND RESULTS

The experimental angular distributions were compared with the predictions of zero-range distorted-wave (DWBA) calculations using the code DWUCK IV.<sup>15</sup> The optical model parameters for  $^3\text{He}$  were triton potentials with spin-orbit terms by Hardekopf, Veeseer, and Keaton,<sup>16</sup> and for the deuterons global fit parameters<sup>17</sup> were used. The parameters are listed in Table I. The captured proton was assumed to be bound by a conventional Woods-Saxon potential well defined by  $r_0 = 1.20$  fm,  $a = 0.75$  fm, and  $\lambda = 25$ . The well depth is adjusted by the code to reproduce the appropriate binding energy. The nonlocality parameters  $\beta = 0.25$  for the  $^3\text{He}$  and  $\beta = 0.54$  for the deuterons were used. In Fig. 2 the calculated angular distributions are shown in comparison with the data. All DWBA calculations yielded angular distributions systematically different from some of the experimental data as was noted earlier<sup>5</sup> in the analysis of the 18 MeV  $^{50,52}\text{Cu}(^3\text{He},d)$  reactions.

Different sets of optical parameters were tested in order to assess the stability of DWBA predictions. In particular, substitution of the global set of Becchetti and Greenlees<sup>18</sup>  $^3\text{He}$  parameters for the parameters of Ref. 16 yielded angular distributions of very similar shapes. However, curves calculated with parameters of Ref. 18 are shifted forward slightly and also show a modest relative enhancement of the small-angle cross section (by 10–20% for  $l = 1$ , and 30–50% for  $l = 3$  transitions) compared to those obtained from parameters of Ref. 16. For comparison calculations made with these two sets for the  $p_{3/2}$  ground state and the  $f_{5/2}$  970 keV level are displayed in Fig. 3. It was also noted that the Becchetti-Greenlees set gives cross sections at the first stripping peak which are smaller than those with the Hardekopf parameters by some 30%. The relative enhancement of cross-sections in the small angle region or an overall shift of angular distributions by one set of parameters relative to another do not interfere with the check for  $j$  dependence, since they appear uniformly for a given orbital angular momentum transfer  $l$ . Neither calculation predicts differences deriving from the total angular momentum transfer,  $j = l + \frac{1}{2}$  and  $j = l - \frac{1}{2}$ . Since we have a spin-zero target nucleus, the measured cross section is related to the calculated DWBA cross section by

$$\left. \frac{d\sigma(\theta)}{d\Omega} \right|_{\text{exp}} = N(2j + 1)C^2S \left. \frac{d\sigma(\theta)}{d\Omega} \right|_{\text{DWBA}},$$

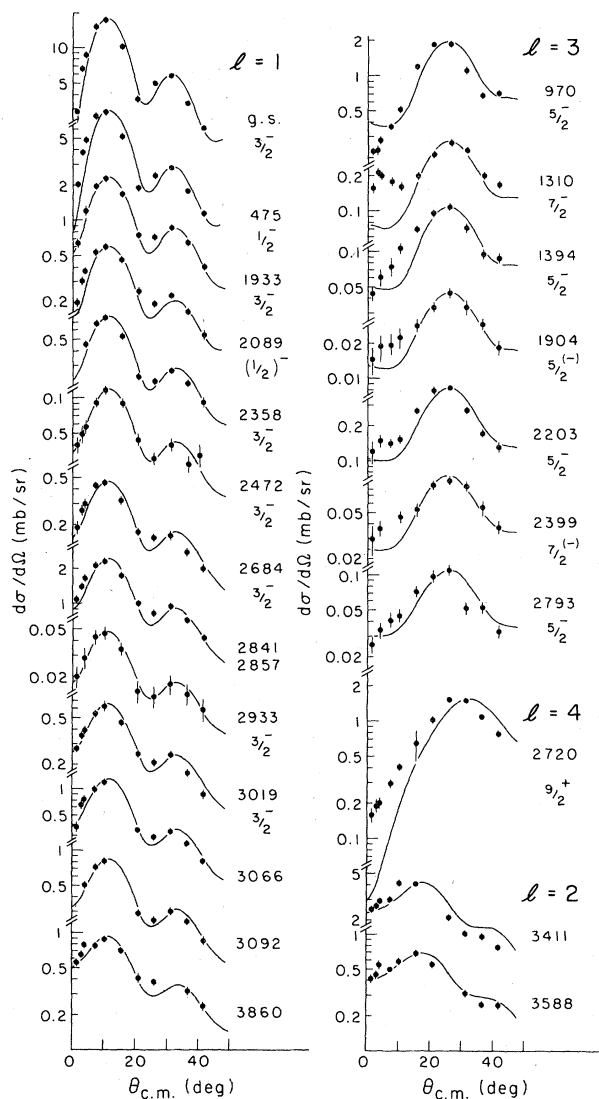


FIG. 2. Angular distributions for  $^{60}\text{Ni}(^3\text{He},d)^{61}\text{Cu}$  at  $E(^3\text{He}) = 18$  MeV up to 3.86 MeV excitation. Error bars contain all known and estimated random errors. Level energies are given in keV. The curves drawn are from DWBA calculations using the parameters listed in Table I (Ref. 16). Level energies and  $J^\pi$  values shown are taken from Ref. 14. Note that all known  $\frac{3}{2}^-$  and  $\frac{7}{2}^-$  transitions tend to agree with the DWBA curves, whereas deviations exist between cross sections of  $\frac{1}{2}^-$  and  $\frac{5}{2}^-$  transitions and DWBA calculations.

where  $j$  is the final-state spin,  $S$  is the spectroscopic factor, and  $C$  is an isospin Clebsch-Gordan coefficient. The value 4.42 has been used as proposed by Bassel<sup>19</sup> for the zero-range normalization factor  $N$ . The extracted spectroscopic strengths and deduced  $l$  values are listed in Table II and are compared with

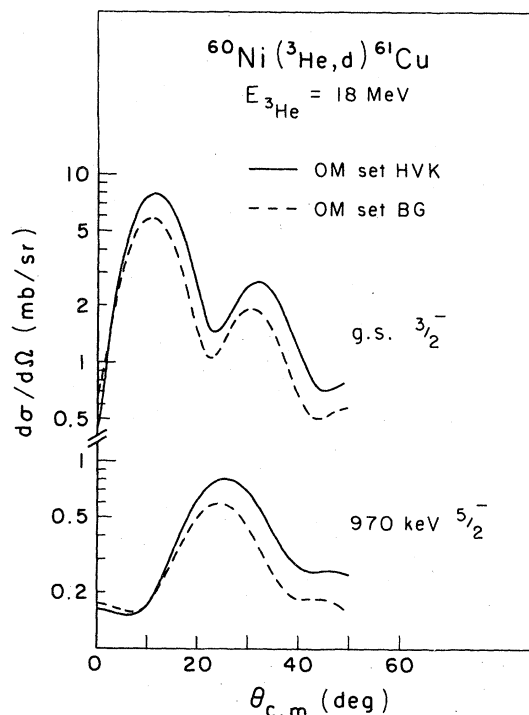


FIG. 3. Comparison of DWBA calculations for the  $^{60}\text{Ni}(^3\text{He},d)^{61}\text{Cu}$  reaction at 18 MeV using the optical model parameters listed in Table I. Solid lines indicate the calculations obtained with the  $^3\text{He}$  parameters by Ref. 16 and the broken lines with parameters of Ref. 18. Note the difference in the predicted magnitudes by two sets of parameters and also the slight difference in the position of the stripping peaks.

previously adopted level properties of Ref. 14 and the results of Ref. 6. A graphical presentation of the deduced spectroscopic strengths is given in Fig. 4.

#### IV. DISCUSSION

##### A. $J$ effects in angular distributions

The structure and  $j$  values of the states in  $^{61}\text{Cu}$  have been extensively investigated by means of proton-capture experiments.<sup>7-12</sup> Adopted  $j$  values in the Nuclear Data Sheets (Ref. 14) for the states in  $^{61}\text{Cu}$  are listed in Table II and shown in Fig. 2 with the measured angular distributions for the present ( $^3\text{He},d$ ) experiment. Table II shows that there are a number of  $^{61}\text{Cu}$  states with firm  $\frac{1}{2}^-$ ,  $\frac{3}{2}^-$ ,  $\frac{5}{2}^-$ , and  $\frac{7}{2}^-$  spin assignments. It was for this reason that the  $^{60}\text{Ni}$  target was one of those chosen for our studies of  $j$  dependence in ( $^3\text{He},d$ ).

More than ten  $l = 1$  and four  $l = 3$  transitions

TABLE I. Optical-model parameters used in  $^{60}\text{Ni}(^3\text{He},d)^{61}\text{Cu}$  calculations.

	$V$ (MeV)	$r_0$ (fm)	$a_0$ (fm)	$W_v$ (MeV)	$4W_D$ (MeV)	$r_I$ (fm)	$a_I$ (fm)	$V_{so}$ (MeV)	$r_{so}$ (fm)	$a_{so}$ (fm)	
18 MeV $^3\text{He}$	165.3	1.20	0.65	16.7	0	1.60	0.80	6.0	1.15	0.63	Ref. 16
	150.5	1.20	0.72	37.2	0	1.40	0.88	6.0	1.20	0.88	Ref. 18
17.6 MeV $d$	92.20	1.15	0.79	0.04	54.95	1.33	0.736	5.5	1.10	0.55	Ref. 17
Bound proton	a	1.20	0.75					$\lambda = 25$			

<sup>a</sup>Well depth adjusted by code to fit proton separation energy.

TABLE II. Spectroscopic results for  $^{61}\text{Cu}$  and comparison with previous work. Spin values in Column 3 indicate the  $j$  value suggested by the  $j$ -dependent effects in the angular distributions and used for the calculation of  $C^2S$  (column 6). Where statistics are too limited to ascertain either a clear systematic disagreement or a good agreement with the DWBA curves this method was not used. Where  $J^\pi$  remains uncertain, the average value for  $C^2S(2J+1)$  is given.

$E_x^a$ (MeV)	Present work $^{60}\text{Ni}(^3\text{He},d)^{61}\text{Cu}$ , $E = 18$ MeV					Nuclear Data Sheets Ref. 14				$^{60}\text{Ni}(^3\text{He},d)$ , $E = 16.4$ MeV Ref. 6		
	$l$	$J^\pi$	$(d\sigma/d\Omega)_{\max}^b$ (mb/sr)	$C^2S$	$C^2S(2J+1)$	$J^\pi$	$E_x$ (MeV)	$l$	$C^2S(2J+1)$			
0	1		17		2.16	$\frac{3}{2}^-$	0	1	0.96			
0.4750	1	$(\frac{1}{2})^-$	8.5	0.48	0.96	$\frac{1}{2}^-$	0.477	1	0.49			
0.9700	3	$(\frac{5}{2})^-$	1.9	0.54	3.26	$\frac{5}{2}^-$	0.972	3	1.0			
1.3104	3	$(\frac{7}{2})^-$	0.38	0.05	0.40	$\frac{7}{2}^-$	1.306	3	0.22			
1.3941	3	$(\frac{5}{2})^-$	0.24	0.06	0.36	$\frac{5}{2}^-$	1.390	3?	0.27			
1.6602						$\frac{3}{2}^-$						
1.7325						$\frac{7}{2}^{(-)}$						
1.9041	3		0.05		0.06	$\frac{5}{2}^{(-)}$						
1.9326	1	$(\frac{3}{2})^-$	2.28	0.06	0.22	$\frac{3}{2}^-$	1.940	1	0.11			
1.9423						$\frac{7}{2}^-$						
2.0887	1	$(\frac{1}{2})^-$	0.60	0.03	0.06	$(\frac{1}{2})^-$	2.104	1	0.03			
2.2032	3	$(\frac{5}{2})^-$	0.42	0.09	0.56	$\frac{5}{2}^-$	2.216	3	0.20			
2.2950						$\frac{9}{2}^-$						
2.3362						$\frac{9}{2}^-$						
2.3581	1		0.78		0.07	$\frac{3}{2}^-$	2.368	1	0.03			
2.3989	3		0.09		0.08	$\frac{7}{2}^{(-)}$	2.390					
2.4723	1	$(\frac{3}{2})^-$	0.12		0.01	$\frac{3}{2}^-$	2.478					
2.5836						$(\frac{7}{2}, \frac{9}{2})$						
2.5845						$(\frac{3}{2}, \frac{5}{2})$						

TABLE II. (Continued).

$E_x^a$ (MeV)	Present work $^{60}\text{Ni}(^3\text{He},d)^{61}\text{Cu}$ , $E = 18$ MeV					Nuclear Data Sheets Ref. 14	$^{60}\text{Ni}(^3\text{He},d)$ , $E = 16.4$ MeV Ref. 6		
	$l$	$J^\pi$	$(d\sigma/d\Omega)_{\text{max}}^b$ (mb/sr)	$C^2S$	$C^2S(2J+1)$	$J^\pi$	$E_x$ (MeV)	$l$	$C^2S(2J+1)$
2.6118						$\frac{9}{2}^-$			
2.6268						$(\frac{11}{2})$	2.629		
2.6840	1		0.46		0.04	$\frac{3}{2}^-$	2.680		
2.7202	4		1.5	0.28	$2.80(\frac{9}{2}^+)$	$(\frac{9}{2}^+)$	2.711	4	1.4
2.7280						$\frac{7}{2}^{(-)}$			
2.7925	3	$(\frac{5}{2})^-$	0.11	0.02	0.13	$\frac{5}{2}^-$	2.794		
2.8406	1	$(\frac{1}{2})^-$	2.3	0.11	0.23	$\frac{1}{2}^-$ , $\frac{3}{2}^-$ , $\frac{5}{2}^-$	2.846	1	0.14
2.8570									
2.9239						$(\frac{9}{2})$			
2.9325	1		0.05		0.004	$\frac{3}{2}^-$	2.942		
3.0015									
3.0156						$(\frac{11}{2})$			
3.0192	1	$(\frac{3}{2})^-$	0.64	0.02	0.06	$\frac{3}{2}^-$	3.019		
3.0655	1		1.1		0.11	$(\frac{3}{2}, \frac{5}{2})$	3.064		
3.0920	1		0.81		0.08	$(\frac{3}{2}, \frac{5}{2})$	3.094		
3.1984									
3.2596						$(\frac{11}{2})$			
3.276 <sup>c</sup>							3.276		
3.3229?									
3.3733?						$(\frac{9}{2})$			
3.411	2		4.2		0.64	$\frac{3}{2}^+$ , $\frac{5}{2}^+$	3.411		
3.437									
3.4544									
3.522						$\frac{1}{2}^-$ , $\frac{3}{2}^-$ , $\frac{5}{2}^-$	3.526		
3.588	2		0.68		0.10		3.588		
3.708 <sup>c</sup>							3.708		
3.790 <sup>c</sup>							3.790		
3.860	1		0.88		0.09		3.860		

<sup>a</sup> The measured excitation energies agree within their uncertainties (of 5 keV) with those adopted in the Nuclear Data Sheets which are quoted here.

<sup>b</sup> Estimated absolute scale error is  $\pm 15\%$ .

<sup>c</sup> Weak state, no angular distribution is obtained in this study due to close impurity peaks at many angles.

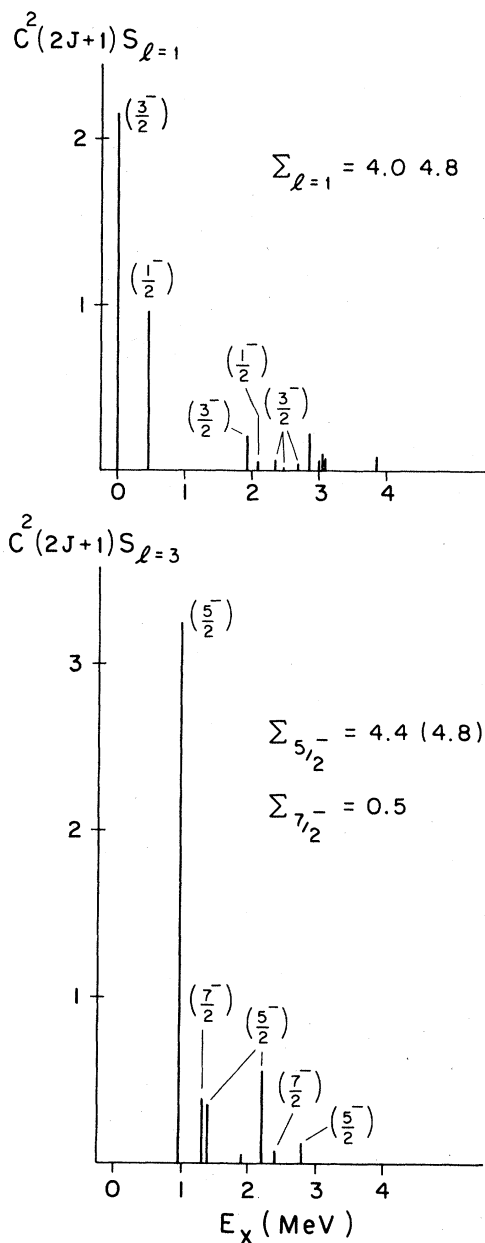


FIG. 4. Graphs of spectroscopic strengths for the  $l = 1$  and  $l = 3$  transfers in  $^{60}\text{Ni}(^3\text{He},d)^{61}\text{Cu}$  up to 3.86 MeV excitation. The average  $C^2S(2J + 1)$  values were used where  $J^\pi$  is uncertain. Theoretical  $C^2S(2J + 1)$  values for  $T_<$  states are given in brackets. For  $l = 3$  the  $f_{5/2}$  and  $f_{7/2}$  strengths are extracted separately. About 8% of the total  $1f_{7/2}$  proton single-particle strength is observed.

are strongly excited and well resolved in the present  $^{60}\text{Ni}(^3\text{He},d)$  experiment. The general agreement between the DWBA predictions and experimentally

obtained angular shapes (see Fig. 2) is of the same quality as in the  $^{50,52}\text{Cr}(^3\text{He},d)$  case,<sup>5</sup> i.e., good agreement is seen for  $f_{7/2}$  and  $p_{3/2}$  transfers, whereas the measured angular distributions for all known  $f_{5/2}$  and  $p_{1/2}$  transfers peak at smaller angles than the calculations. For a better illustration of this effect the strongest  $l = 1$  and  $l = 3$  angular distributions are shown in enlarged scale in Fig. 5. They are compared with similar transitions<sup>5</sup> for  $^{50}\text{Cr}(^3\text{He},d)^{51}\text{Mn}$ . The dashed curves in Fig. 5 are similar to the solid (DWBA) curves, but displaced forward by about  $2.5^\circ$ . Such a shift produces a much improved fit to the  $f_{5/2}$  and  $p_{1/2}$  transfers in  $^{61}\text{Cu}$  as well as in  $^{51}\text{Mn}$ . We refer to this "shift" of the stripping peak as the small-angle  $j$  effect. Of seven  $l = 1$  transfers in  $^{60}\text{Ni}(^3\text{He},d)^{61}\text{Cu}$  with a firm spin assignment  $j^\pi = \frac{3}{2}^-$  five levels (at 0, 1933, 2358, 2684, and 3019 keV) are strongly excited and are measured with good statistics. The level at 475 keV has a definite assignment  $j^\pi = \frac{1}{2}^-$  and can be used for a comparison of its angular shape

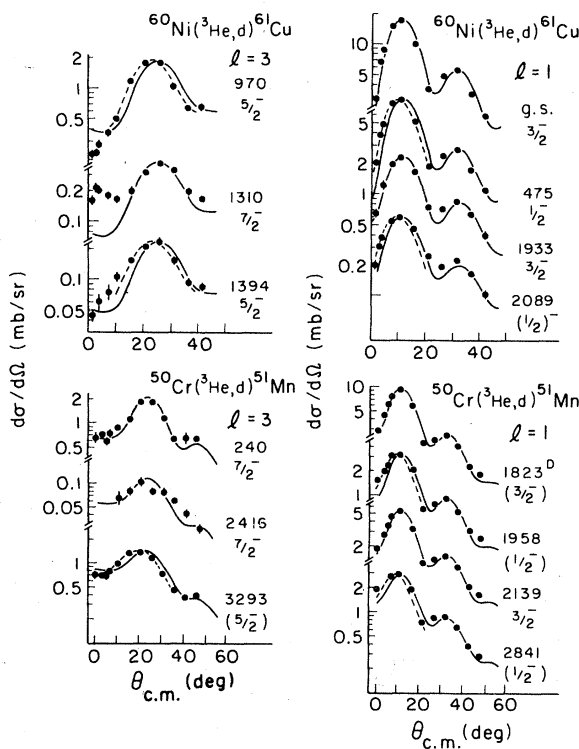


FIG. 5. Comparison of the small-angle  $j$  effects in  $^{60}\text{Ni}(^3\text{He},d)^{61}\text{Cu}$  and  $^{50}\text{Cr}(^3\text{He},d)^{51}\text{Mn}$  for known and strong  $l = 1$  and 3 transitions. The solid lines are DWBA calculations. The dashed lines are drawn to emphasize the shift of the stripping peaks observed for  $p_{1/2}$  and  $f_{5/2}$  transitions.

with those of the  $\frac{3}{2}^-$  states. A second level, at 2089 keV, has been tentatively adopted as  $\frac{1}{2}^-$ . This level and the 475 keV level had been assigned  $\frac{1}{2}^-$  on the basis of  $p-\gamma$  angular correlations<sup>9,11</sup> in  $^{58}\text{Ni}(\alpha,\gamma)$ . This study also suggested spin  $\frac{1}{2}^-$  for the state at 2841 keV, one member of the unresolved ( $l=1$ ) doublet which was observed as a broad peak at all angles in our work.

We find that when the angular distributions rise or fall steeply the DWBA fit to the data seems to get worse. For such cases the  $j$  dependence can be obscured by the poor fit. Even so, deviations from the DWBA predictions for the cross section of the 475 and 2089 keV levels ( $\frac{1}{2}^-$ ) are at least a factor of 2 larger than for those of the g.s. ( $\frac{3}{2}^-$ ) at small angles ( $\theta \leq 5^\circ$ ). This effect is seen more quantitatively if we plot the data points divided by their DWBA predictions, as in Fig. 6. A careful inspection shows that the DWBA curves remain in good agreement with the  $\frac{3}{2}^-$  transfer data as the excitation energy increases, while the small angle ( $\theta \leq 5^\circ$ ) cross sections of the  $\frac{1}{2}^-$  states at 475, 2089, and 2841 keV are about 40% larger than predicted by DWBA. One exceptional angular behavior is noticed for the level at 2684 keV. Hoffman *et al.*<sup>11</sup> suggested a  $J^\pi$  values of  $\frac{3}{2}^-$  for this level in their  $p-\gamma$  decay study. But in contrast with other  $\frac{3}{2}^-$  levels its small angle ( $\theta \leq 5^\circ$ ) cross sections are enhanced by about 20% on the average. This difference from DWBA is larger than for the other  $p_{3/2}$  transitions but only half that of the  $p_{1/2}$  states. Since the level density at 2.6 MeV is fairly high, contributions from a second, unresolved level are considered likely.

For  $l=3$  states  $j$  values have been established in Refs. 9–12 and references therein:  $\frac{5}{2}^-$  for the levels at 970, 1394, 2203, and 2793 keV and  $\frac{7}{2}^-$  for the 1310 keV level. For the level at 2399 keV a  $\frac{7}{2}^-$  assignment was proposed<sup>11</sup> and confirmed on the basis of transition correlations<sup>12</sup> which excluded other spin values for this level. Again, the experimental angular distributions for the known  $f_{5/2}$  to  $^{61}\text{Cu}$  levels, especially those at 970, 1394, and 2203 keV, which have relatively large cross sections, exhibit a forward shift of their stripping cross peaks by about  $3^\circ$  relative to their calculated DWBA curves. The experimental angular shape of the  $f_{7/2}$  state at 1310 keV is less peaked than those of nearby  $f_{5/2}$  states and the agreement with the DWBA predictions is fairly good at the stripping peak. The level at 2399 keV ( $\frac{7}{2}^-$ ) which is not as strong as the one at 1310 keV shows the same  $f_{7/2}$  feature. As seen in

Fig. 5 this difference between transitions to  $\frac{5}{2}^-$  and  $\frac{7}{2}^-$  states was also observed in our ( $^3\text{He},d$ ) studies on the chromium isotopes. Therefore the existence of an  $l=3$   $j$  dependence in the ( $^3\text{He},d$ ) reaction finds additional support from the forward shift of these three known  $f_{5/2}$  transitions in  $^{61}\text{Cu}$ . We see two  $l=2$  and one  $l=4$  positive parity transitions

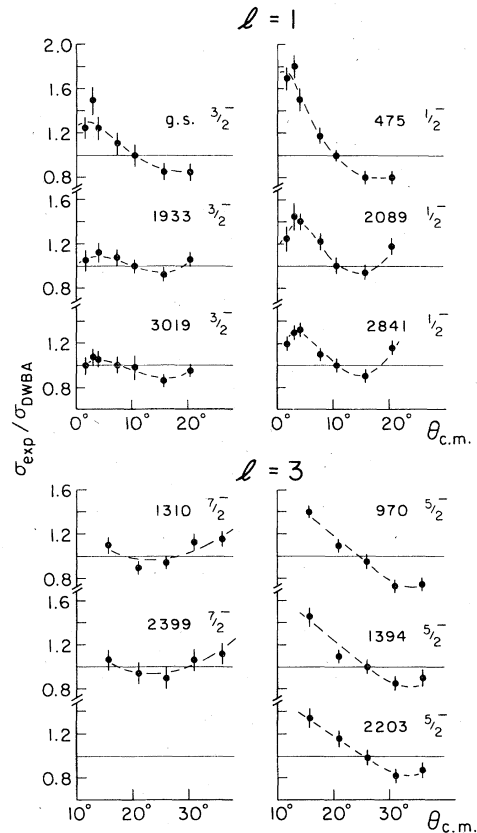


FIG. 6. Ratio of experimental to DWBA cross sections for the region within  $\pm 10^\circ$  of the stripping peaks. The  $^{61}\text{Cu}$  levels are labeled by their excitation energy in keV. Calculations are normalized to the data at the computed stripping peaks ( $\theta=10^\circ$  for  $l=1$ ;  $\theta=25^\circ$  for  $l=3$ ). Error bars include all uncertainties from statistics, monitoring, and background subtractions. The ratio demonstrate that for  $p_{3/2}$  and  $f_{7/2}$  transfer the data typically agree with DWBA results to within about 10%, i.e., almost within experimental errors. The forward shift seen for  $p_{1/2}$  and  $f_{5/2}$  transfer in Fig. 2 now appears as a forward angle enhancement of the  $j=l-\frac{1}{2}$  transfers by factors of 1.3 to 1.4, i.e., by up to 5 standard deviations. For  $l=1$  transfers, in addition to the  $j$  effect, the  $Q$ -value dependence of the cross sections is not fully explained by our calculations. Lines are drawn to guide the eye.

up to 3.9 MeV excitation energy in  $^{61}\text{Cu}$ . No definite spin has been assigned for the strong  $l = 2$  state at 3411 keV. The weaker  $l = 2$  transfer at 3588 keV has been newly identified in this ( $^3\text{He},d$ ) study. Since contaminant peaks are located close to these two states at most angles, their cross sections reflect the additional uncertainties arising from the separation of the peaks. The  $l = 4$  transfer at 2720 keV is strong, and its angular distribution shows a  $4-5^\circ$  forward shift compared to the DWBA curve. This level is assigned as  $\frac{9}{2}^+$  in Refs. 11 and 12.

### B. Spectroscopy of $^{61}\text{Cu}$

Up to 3.9 MeV excitation and 23 levels were analyzed. The spectroscopic strengths  $C^2S(2J+1)$  are listed in Table II and are also in Fig. 4. Of the strengths theoretically expected for  $T_<$  states,<sup>20</sup> 83% for  $l = 1$  and 92% for  $f_{5/2}$  are observed in this work. The observed  $f_{7/2}$  stripping strength is still 0.48, indicating an imperfect closure of the  $f_{7/2}$  shell in  $^{60}\text{Ni}$ . The missing  $l = 1$  strength is expected to be found in levels beyond  $E^* = 3.9$  MeV (see Fig. 4 and Table 3 in Ref. 6). Our spectroscopic factors extracted with the use of optical-model parameters by Hardekopf *et al.*<sup>16</sup> are about twice as high as the values given in Ref. 6 (see the last column of Table II). A similar disagreement was observed by Fuchs *et al.*<sup>21</sup> who stated in their  $^{60}\text{Ni}(d,n)$  study that the spectroscopic strengths of Ref. 6 are probably too low by about a factor of 3. The use of Becchetti and Greenlees  $^3\text{He}$  optical-model parameters in our analysis would give about 20% higher spectroscopic factors for our data.

Our observed  $l_p$  transfers are in perfect agreement with existing assignments. In Table II it can be seen that our  $j$  values (in column 2) suggested on the basis of small angle deviations from DWBA for  $l = 3$  transfers agree very well with previously adopted values.<sup>14</sup> We note that many high-spin states as well as the levels at 1.660( $\frac{3}{2}^-$ ) and 1.942( $\frac{7}{2}^-$ ) MeV are not excited in this study. In comparison with the results of Ref. 6 a number of points can be made. Three  $l = 3$  transitions are newly observed at 1.904, 2.399( $\frac{7}{2}^-$ ), and 2.793( $\frac{5}{2}^-$ ) MeV. Seven additional  $l = 1$  level distributions are measured at 2.472, 2.684, 2.933, 3.019, 3.066, 3.860 MeV. The level at 3.411 MeV, tentatively assigned as an  $l = 2$  state in Ref. 6, has been confirmed as  $l = 2$  and another, new  $l = 2$  level is seen at 3.588 MeV. The  $l = 4$  transition to

the 2.720 MeV level assigned as  $\frac{9}{2}^+$  by Hoffman *et al.*<sup>11</sup> takes about 35% of the total  $1g_{9/2}$  strength.

### V. CONCLUSIONS

It has been found that the small-angle  $j$  dependence of the ( $^3\text{He},d$ ) reaction at 18 MeV, which has been observed for the  $l = 1$  and 3 transfers in the  $^{50,52}\text{Cr}(^3\text{He},d)$  data, is also seen in the present  $^{60}\text{Ni}(^3\text{He},d)$  experiment. In both studies experimental cross sections and DWBA predictions are in good agreement for the  $p_{3/2}$  and  $f_{7/2}$  transfers while they differ systematically for the  $p_{1/2}$  and  $f_{5/2}$  transitions. Evidence for the  $l = 3$   $j$  dependence now becomes more definitive as the angular distributions of all known  $f_{5/2}$  transfers to  $^{61}\text{Cu}$  levels consistently exhibit the  $j$  dependence suggested previously. For  $l = 1$  transitions the  $j$ -dependent effect on angular distributions is the same qualitatively, though not as visible as for the chromium targets. Combining the results of this study and the previous  $^{50,52}\text{Cr}(^3\text{He},d)$   $^{51,53}\text{Mn}$  reactions, we reaffirm the suggestion of Ref. 5 that the small-angle  $j$  dependence in the ( $^3\text{He},d$ ) reaction appears to be a systematic effect, and could be used, at least in the  $f_{7/2}$  shell, to suggest previously unknown  $J^\pi$  values of states populated in proton stripping.

We note that the type of  $j$  dependence reported here (and in Ref. 5) significantly affects the cross section very close to the stripping maximum (compare Fig. 5). These effects are neither predicted nor reproducible in conventional zero-range DWBA calculations. It is conceivable that the mechanism responsible for the  $j$ -dependent angle shifts would also affect the magnitude of the stripping peaks (hence the spectroscopic factors extracted) in a non-trivial way. In ( $d,p$ ) and ( $p,d$ ) reactions similar small-angle  $j$  effects have been seen for  $l = 3$ . Extensive calculations by Kishida and Ohnuma<sup>22</sup> involving the inclusion of the deuteron  $D$  state and exact finite range DWBA calculations produced small corrections of the type needed but failed to yield the magnitude of the observed  $l = 3$   $j$  effect in the energy range from 14 to 30 MeV. An improved theoretical treatment of stripping reactions may be necessary.

### ACKNOWLEDGMENTS

We would like to thank Ms. A. M. Hernandez for her help in data taking. This work was supported by the National Science Foundation.

- \*Present address: Jeonbug National University, Jeonju, Jeonbug, Korea.
- <sup>1</sup>L. L. Lee and J. P. Schiffer, Phys. Rev. Lett. 12, 108 (1964); Phys. Rev. B 136, 405 (1964).
- <sup>2</sup>R. Sherr, E. Rost, and M.E. Rickey, Phys. Rev. Lett. 12, 420 (1964).
- <sup>3</sup>R. H. Fulmer and W. W. Daehnick, Phys. Rev. Lett. 12, 455 (1964); Phys. Rev. 139, B579 (1965).
- <sup>4</sup>W. W. Daehnick, Phys. Rev. 177, 1763 (1969).
- <sup>5</sup>J. E. Park, W. W. Daehnick, and M. J. Spisak, Phys. Rev. C 19, 42 (1979).
- <sup>6</sup>D. J. Pullen and B. Rosner, Phys. Rev. 170, 1034 (1968).
- <sup>7</sup>J. W. Butler and C. R. Gosset, Phys. Rev. 108, 1473 (1957).
- <sup>8</sup>C. R. Gosset and L. S. August, Phys. Rev. 137, B381 (1965).
- <sup>9</sup>E. J. Hoffman and D. G. Sarantites, Nucl. Phys. A157, 584 (1970).
- <sup>10</sup>B. Heusch, B. Cujec, R. Dayras, J. N. Mo, and I. M. Szöghy, Nucl. Phys. A169, 145 (1971).
- <sup>11</sup>E. J. Hoffman, D.G. Sarantites, and N. -H. Lu, Nucl. Phys. A173, 146 (1971).
- <sup>12</sup>D. G. Sarantites, J. H. Barker, N. -H. Lu, E. J. Hoffman, and D. M. Van Patter, Phys. Rev. C 8, 629 (1973).
- <sup>13</sup>M. J. Spisak and W. W. Daehnick, Nucl. Instrum. Methods 153, 365 (1978).
- <sup>14</sup>R. L. Auble, Nucl. Data Sheets 16, No. 1, 11 (1975).
- <sup>15</sup>P. D. Kunz, University of Colorado (unpublished).
- <sup>16</sup>R. A. Hardekopf, L. R. Vesser, and P. W. Keaton, Jr., Phys. Rev. Lett. 35, 1623 (1975).
- <sup>17</sup>J. Childs, PH.D. thesis, University of Pittsburgh, 1976 (unpublished). See potential "E" in W. W. Daehnick, J. Childs, and Z. Vrcelj, Phys. Rev. C 21, 2253 (1980).
- <sup>18</sup>F. D. Becchetti and G. W. Greenlees, *Proceedings of the Third International Symposium on Polarization Phenomena in Nuclear Reactions, Madison, Wisconsin, 1970*, edited by H. H. Barschall and W. Haerberli (University of Wisconsin, Madison, 1971), p. 682.
- <sup>19</sup>R. H. Bassel, Phys. Rev. 149, 791 (1966).
- <sup>20</sup>J. B. French and M. H. Macfarlane, Nucl. Phys. 26, 168 (1961).
- <sup>21</sup>H. Fuchs, K. Grabish, and G. Röscher, Nucl. Phys. A133, 385 (1969).
- <sup>22</sup>N. Kishida and H. Ohnuma, Proceedings of the INS International Symposium on Nuclear Direct Reaction Mechanism, Shikanoshima, Fukuoka, 1978, p. 221.